ISSN 1810-2328, Journal of Engineering Thermophysics, 2017, Vol. 26, No. 1, pp. 79–90. © Pleiades Publishing, Ltd., 2017.

A Numerical Study of Laminar Natural Convective Heat Transfer inside a Closed Cavity with Different Aspect Ratio

S. Das and P. Bhattacharya*

Department of Mathematics, NIT Agartala, PIN 799046 India

Received August 26, 2014

Abstract—Two-dimensional steady-state laminar natural convection was studied numerically for differentially heated air-filled closed cavity with adiabatic top and bottom walls. The temperature of the left heated wall and cooled right wall was assumed to be constant. The governing equations were iteratively solved using the control volume approach. In this paper, the effects of the Rayleigh number and the aspect ratio were examined. Flow and thermal fields were exhibited by means of streamlines and isotherms, respectively. Variations of the maximum stream function and the average heat transfer coefficient were also shown. The average Nusselt number and was correlated to the Rayleigh number based on curve fitting for each aspect ratio. The investigation covered the range $10^4 \leq \mathrm{RA} \leq 10^7$ and is done at Prandtl number equal to 0.693. The result shows the average Nusselt number is the increasing function of Rayleigh number. As the aspect ratio increases, Nusselt number decreases along the hot wall of the cavity. As Rayleigh number increases, Nusselt number increases. Result indicates that at constant aspect ratio, with increase in Rayleigh number the heat transfer rate increases.

DOI: 10.1134/S181023281701009X

1. INTRODUCTION

Natural convection in enclosures is a topic of contemporary importance because enclosures filled with fluid are central components in a long list of engineering and geophysical systems with various geometries. The flow and heat transfer induced, for example, in the air space of a double-pane window system differs fundamentally from the external natural convection in which the boundary layer was considered. The understanding of the recirculation flow and heat transfer within the enclosure is considered as one of the fundamental challenges of computational fluid research. There have been numerous investigations conducted on natural convection in empty cavities under various configurations and boundary conditions [1–3]. Buoyancy-induced flows are more complex because of the coupling between the flow and transport. The first unified and comprehensive review of this subject was done by Ostrach [4, 5]. Lo et al. studied convection in cavities heated from the left vertical wall and cooled from the opposite vertical wall with both horizontal walls insulated using a differential quadrature method. Numerical results are reported for several values of width-to-height aspect ratio of enclosure and Rayleigh number [6]. Basak et al. have studied the effect of uniform and nonuniform temperature at the bottom wall on natural convection in a square cavity for Rayleigh numbers from 10^3 to 10^5 using Galarkin finite element method [7]. They reported that the uniform temperature gives more heat transfer than the nonuniform temperature. Natural convection is discussed in detail for uniform heating at below or side of the square cavity in references [8–15]. Corcione studied natural convection in a rectangular cavity heated from below and cooled from top as well as sides for variety of thermal boundary conditions. Numerical results are reported for several values of both aspect ratios of enclosure and Rayleigh numbers [16]. The objective of this paper is to document the numerical data of steady-state laminar natural convective heat transfer inside closed cavities filled with air having heated left wall and cooled right wall for the range of RA from 10^4 to 10^7 for aspect ratios ranging from 1 to 3. The top and bottom walls of the cavities are adiabatic. The cavity illustrated in Fig. 1 is chosen for simulating natural convective flow and heat transfer characteristics. It consists of dimensions $L \times H$. The gravitational force is acting downwards. The aspect ratio of the cavity is defined as H/L. The top and bottom walls are adiabatic.

*E-mail: p_bhattacharya2001@yahoo.co.in

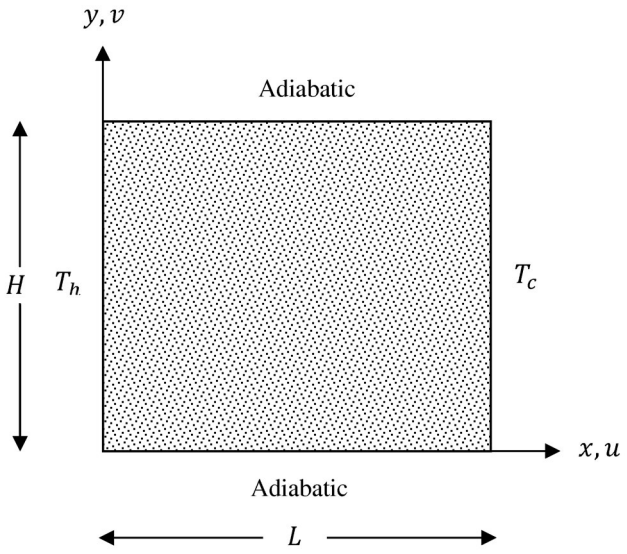

Fig. 1. Geometry of the cavity.

2. MATHEMATICAL FORMULATION

The cavity of length (L) and height (H) has a hot left wall and cold right wall at constant temperatures T_h and T_c, respectively. The top and bottom walls are adiabatic. The gravitational force is acting downwards. A buoyancy flow develops because of thermally induced density gradient. Heat is transferred from the hot wall to the cold wall. The governing equations for the natural convection flow are conservation of mass, momentum and energy and can be written as:

Continuity:

$$\frac{\partial u}{\partial x} + \frac{\partial v}{\partial y} = 0. \tag{1}$$

X-momentum:

$$u\frac{\partial u}{\partial x} + v\frac{\partial v}{\partial y} = -\frac{1}{\rho}\frac{\partial p}{\partial x} + v\left(\frac{\partial^2 u}{\partial x^2} + \frac{\partial^2 u}{\partial y^2}\right). \tag{2}$$

Y-momentum:

$$u\frac{\partial u}{\partial x} + v\frac{\partial v}{\partial y} = -\frac{1}{\rho}\frac{\partial p}{\partial y} + v\left(\frac{\partial^2 v}{\partial x^2} + \frac{\partial^2 v}{\partial y^2}\right) + g\beta(T - T_c). \tag{3}$$

Energy equation:

$$u\frac{\partial T}{\partial x} + v\frac{\partial T}{\partial y} = \alpha\left(\frac{\partial^2 T}{\partial x^2} + \frac{\partial^2 T}{\partial y^2}\right). \tag{4}$$

Rayleigh number:

$$\mathrm{RA} = \frac{g\beta L^3(T_h - T_c)}{\alpha v}.$$

These variables have their common meaning in fluid dynamics and heat transfer as listed in the nomenclature. The thermophysical properties of air are evaluated at the reference temperature that is the

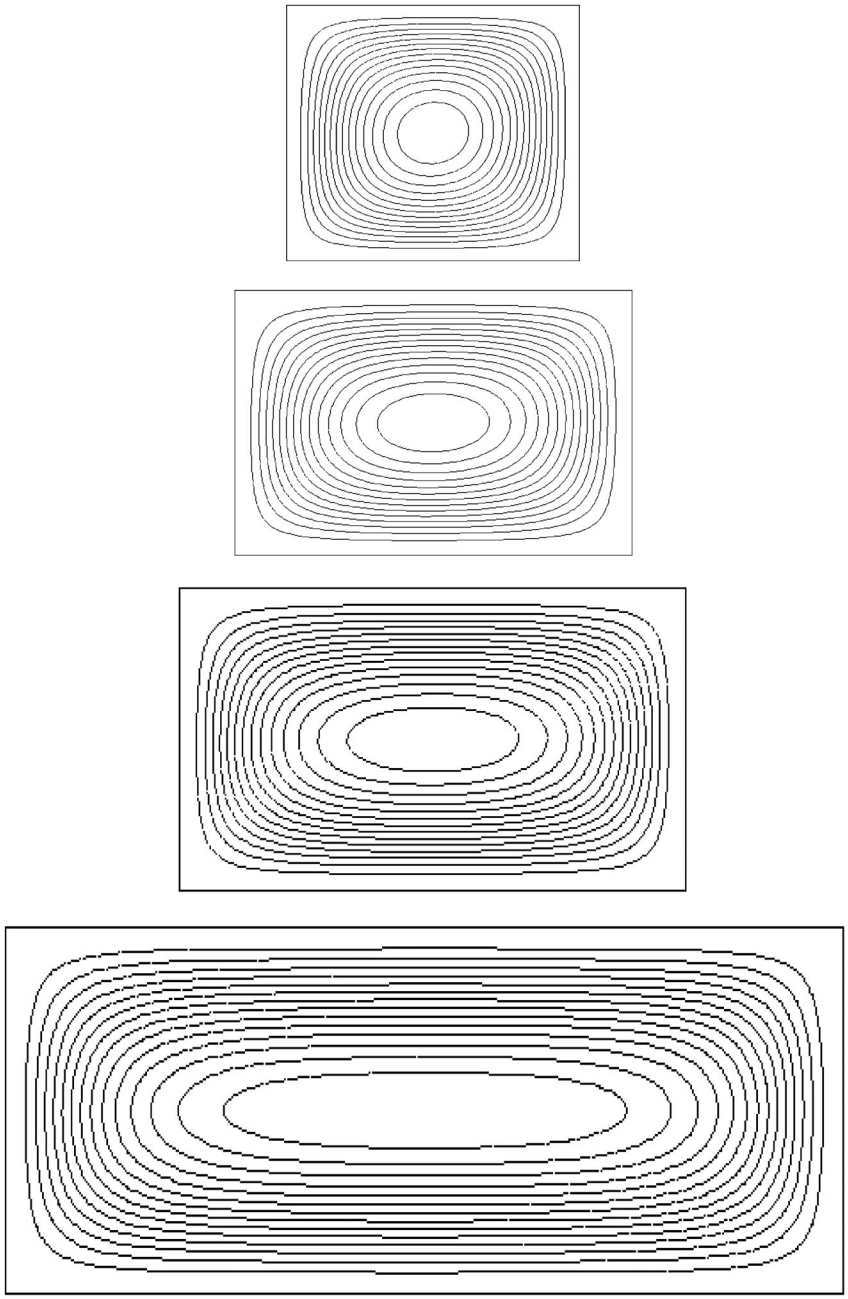

Fig. 2. Streamlines of aspect ratio AR $= 1, 1.5, 2, 3$ at RA $= 2 \times 10^4$.

average of the two wall temperatures. In this study with $Pr = 0.693$ the effects of the Rayleigh number, which is varied from 10^4 to 10^7, are of great interest.

Boundary conditions:

Temperature:

$$\text{at the left wall} \qquad T(0, y) = T_h,$$

$$\text{at the right wall} \qquad T(L, y) = T_c,$$

$$\text{at the top wall} \qquad \frac{\partial T}{\partial y}(x, H) = 0,$$

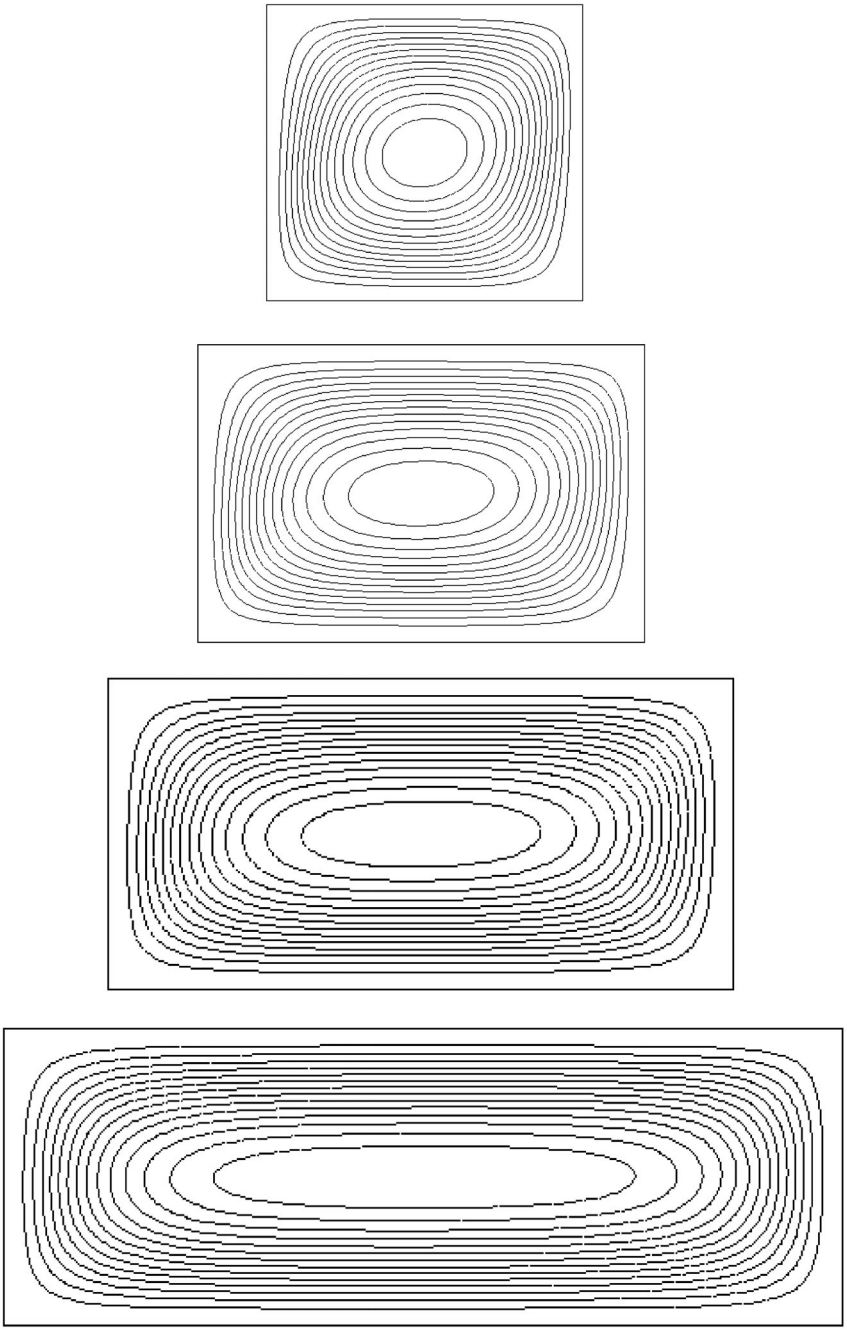

Fig. 3. Streamlines of aspect ratio AR $= 1, 1.5, 2, 3$ at RA $= 3.5 \times 10^5$.

$$\text{at the bottom wall} \quad \frac{\partial T}{\partial y}(x,0) = 0.$$

Velocity:

$$u(x,0) = u(x,L) = u(0,y) = u(L,y) = 0,$$

$$v(x,0) = v(x,L) = v(0,y) = v(L,y) = 0.$$

Here x and y are the distances measured along the horizontal and vertical directions, respectively; u and v are velocity components in the x and y directions, respectively; T denotes the temperature; p is the

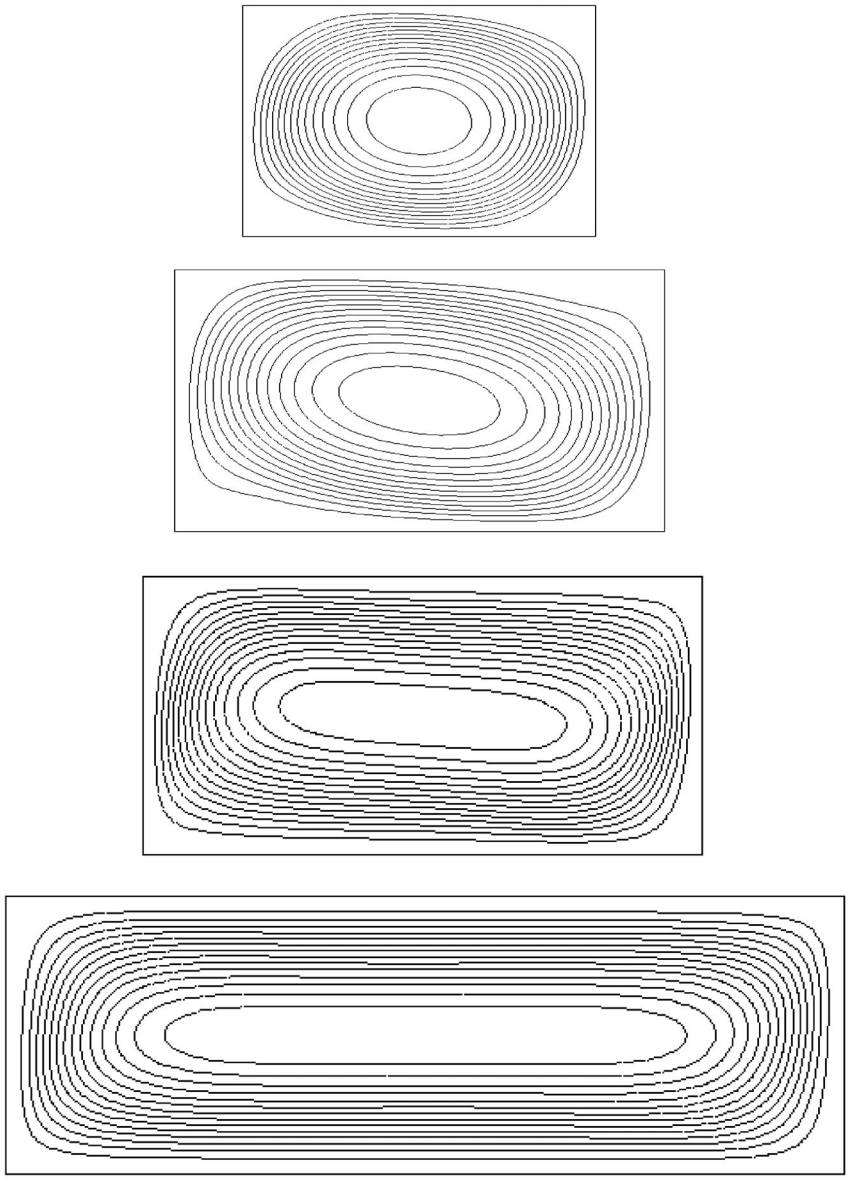

Fig. 4. Streamlines of aspect ratio AR $= 1, 1.5, 2, 3$ at RA $= 5 \times 10^6$.

pressure and ρ is the density; T_h and T_c are the temperatures at the hot and cold walls, respectively; L is the length of the cavity and H is the height of the cavity.

3. NUMERICAL SCHEME

In the present investigation, the set of governing equations is integrated over the control volumes, which produces a set of algebraic equations. The SIMPLE algorithm is used to solve the coupled system of governing equations. Discretization of the momentum and energy equations is performed by a second-order upwind scheme and pressure interpolation is provided by PRESTO scheme. Convergence criterion considered as residuals is admitted 10^{-3} for momentum and continuity equations, and for the energy equation it is lower than 10^{-6}. The calculations are carried out using the FLUENT 6.3 commercial code. The uniform grid system of 110×110 is adopted here.

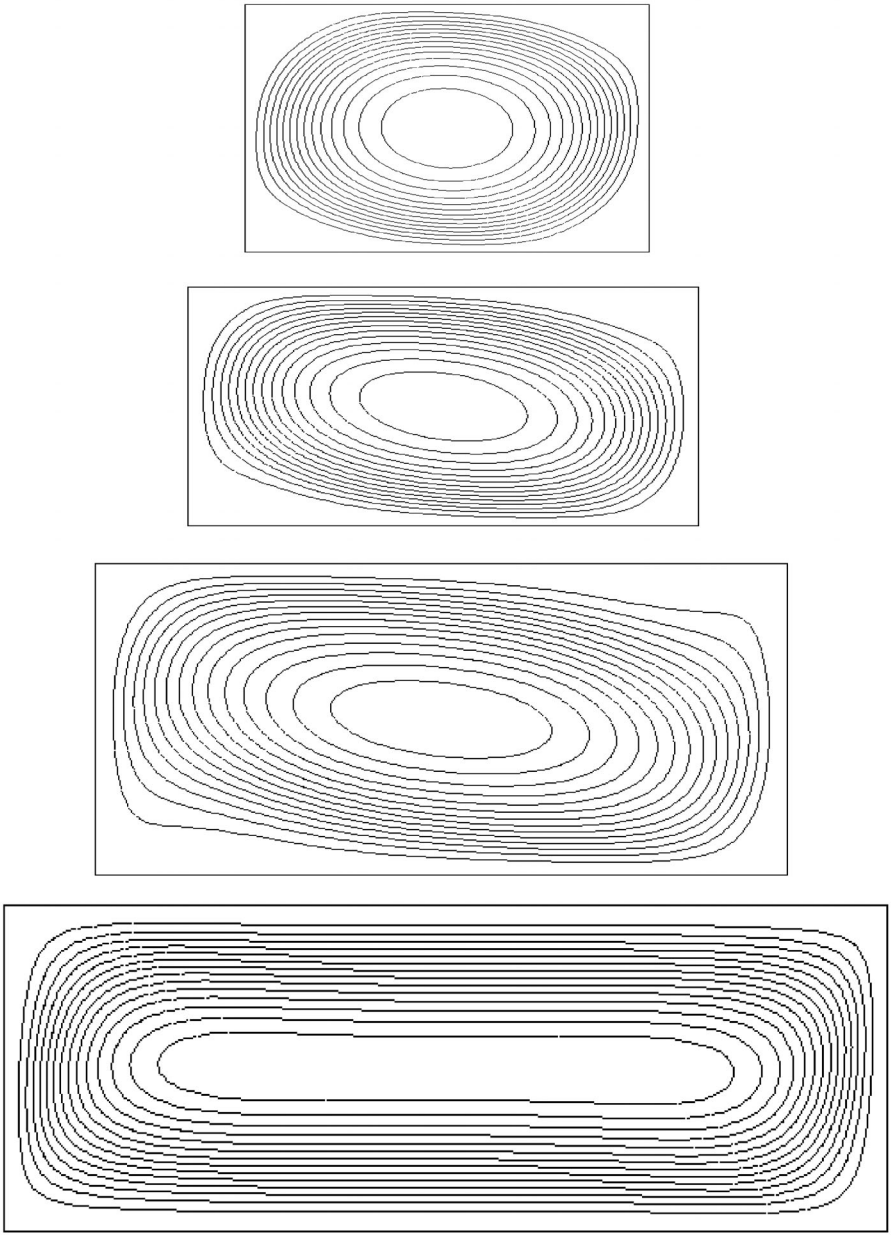

Fig. 5. Streamlines of aspect ratio $\mathrm{AR} = 1, 1.5, 2, 3$ at $\mathrm{RA} = \times 10^7$.

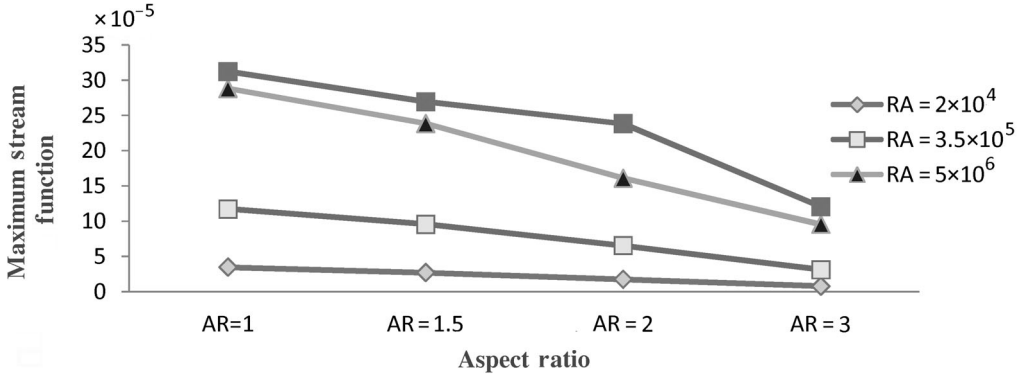

Fig. 6. The maximum value of the stream function for different aspect ratio and Rayleigh numbers.

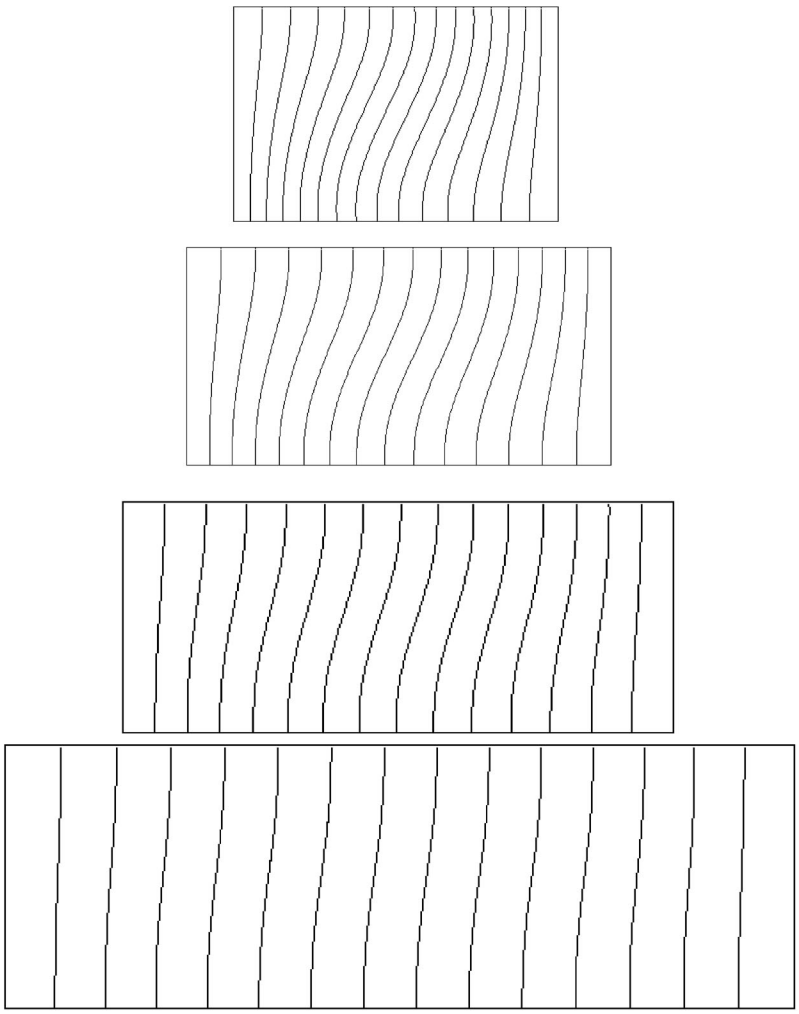

Fig. 7. Isotherms of aspect ratio AR $= 1, 1.5, 2, 3$ at RA $= 2 \times 10^4$.

4. RESULTS AND DISCUSSION

Cases with the vertical left hot wall of the closed cavity were studied here. The effects of the Rayleigh number and aspect ratio $L/H = 1, 1.5, 2, 3$ were systematically investigated. Comparisons of the flow field and overall heat transfer rates among different aspect ratios were presented.

4.1. Effects of Rayleigh Number

4.1.1. Flow Patterns and Flow Intensity

The flow fields are shown by means of streamlines shown below. Due to the buoyant effects caused by the temperature difference between the left hot wall and right cold wall, recirculating vortices are formed, which are clearly demonstrated by the closed streamlines.

In the above figures we observe that at different values of RA as the aspect ratio increases the central vortices change the shape from circular to ellipse. As Rayleigh number increases, streamlines become more densely packed next to the walls. Also, at constant values of the aspect ratio as RA increases, the core of the vortices becomes larger.

On the other hand, the flow intensity is examined through the maximum value of the dimensionless stream function, $\Psi_{\max}$, whose variation versus the Rayleigh number is shown in Fig. 6. As expected, the maximum steam function is significantly increased with increased Rayleigh number due to enhanced

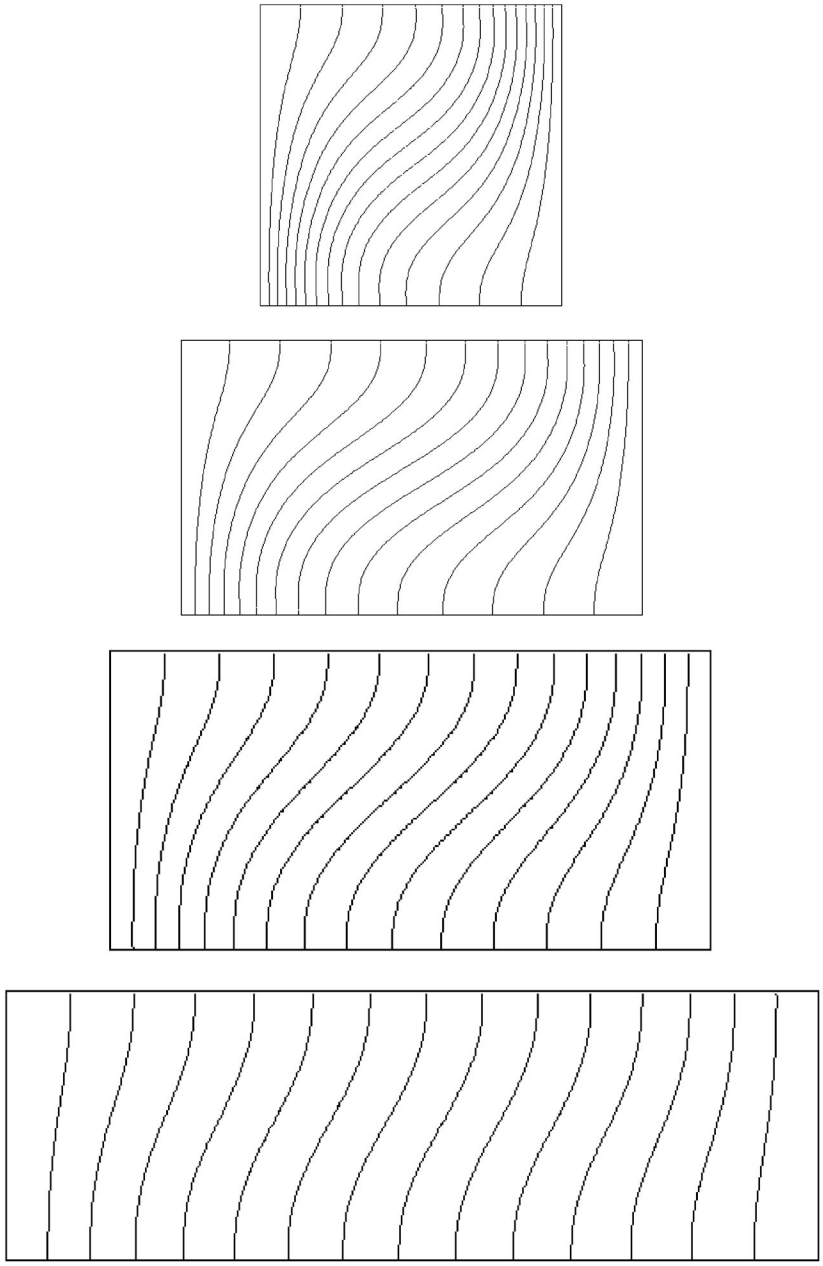

Fig. 8. Isotherms of aspect ratio AR $= 1, 1.5, 2, 3$ at RA $= 3.5 \times 10^5$.

buoyancy-driven convection. Since the Rayleigh number is based on the length (L) of the closed cavity. Therefore, at constant Rayleigh number, the maximum stream function becomes greater as the aspect ratio L/H is decreased due to enlarged flow area. As indicated by Moukalled and Acharya [17], the increment of the flow area also enhances the various frictions that tend to decay the flow intensity. As Rayleigh number increases, the enhanced natural convection becomes dominant and the additional friction is negligible, leading to that the maximum stream functions at lower aspect ratio are apparently greater than those at higher aspect ratios.

4.1.2. Heat Transfer

The thermal fields are presented in the form of isotherms in figures shown below with the same arrangement as in Figs. 2–5. The isotherms pattern reveals that as Rayleigh number increases, the packing of isotherms near the active walls becomes prominent implying rise in Nusselt number. The

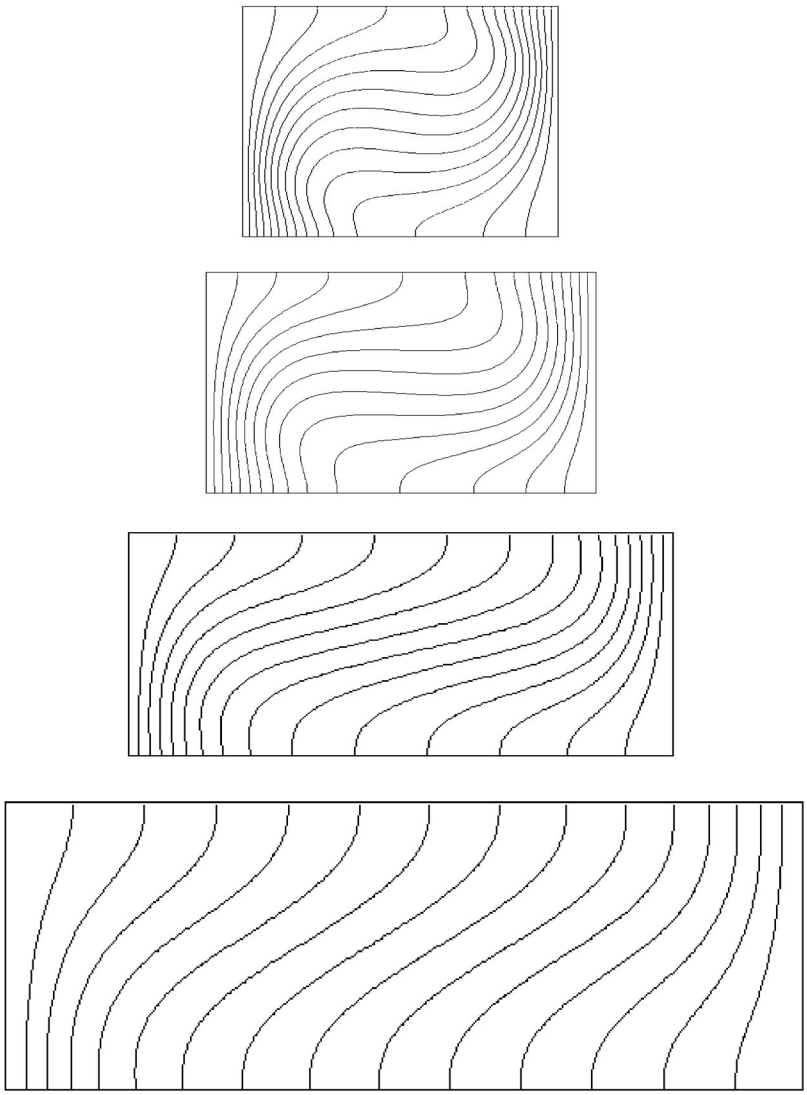

Fig. 9. Isotherms of aspect ratio AR $= 1, 1.5, 2, 3$ at RA $= 5 \times 10^6$.

isotherms are orthogonal at the insulated walls, ensure that the heat transfer rate becomes zero. As Rayleigh number increases, the heat transfer rate increases, velocity increases, and the isotherms are no longer orthogonal, they bend.

Variations of the average heat transfer coefficient along the hot wall of the cavity for different aspect ratios and Rayleigh number are plotted in Fig. 11. As Rayleigh number increases, the heat transfer rate along the hot wall of the cavity increases at constant aspect ratio, but at constant Rayleigh number the heat transfer rate along the same wall decreases as the aspect ratio increases.

4.2. Correlation of Average Nusselt Number with Rayleigh Number

The variations of average Nusselt numbers for different aspect ratios and Rayleigh numbers are plotted in the graph shown below in Fig. 12. Thus, the obtained equations that demonstrate the behavior of the Nusselt number as a function of Rayleigh number are given in the table.

5. CONCLUSIONS

A numerical study on steady laminar natural convective heat transfer inside a closed cavity filled with air was carried out. The effects of Rayleigh number, aspect ratio on the flow and heat transfer were systematically studied. From the result and discussion we conclude that as Raleigh number increases,

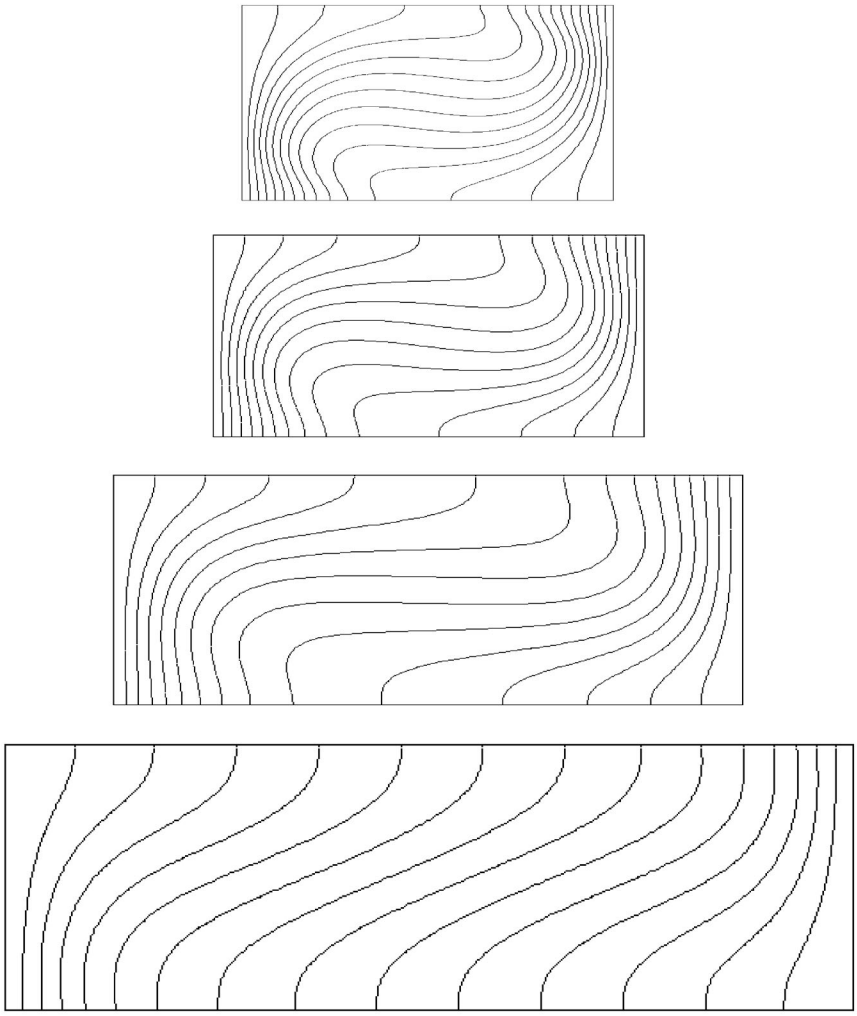

Fig. 10. Isotherms of aspect ratio AR = 1, 1.5, 2, 3 at RA = 10^7.

Correlation of average Nusselt number with Rayleigh number

AR = 1	AR = 1.5	AR = 2	AR = 3
$\overline{Nu} = 0.239\mathrm{RA}^{0.139}$	$\overline{Nu} = 0.126\mathrm{RA}^{0.163}$	$\overline{Nu} = 0.110\mathrm{RA}^{0.147}$	$\overline{Nu} = 0.164\mathrm{RA}^{0.072}$
$\mathrm{RA}^2 = 0.872$	$\mathrm{RA}^2 = 0.886$	$\mathrm{RA}^2 = 0.832$	$\mathrm{RA}^2 = 0.756$

streamlines become more densely packed next to the walls. Also, at constant values of aspect ratio as RA increases the core of the vortices becomes larger. As Rayleigh number increases, the enhanced natural convection becomes dominant and the additional friction is negligible, leading to that the maximum stream functions at lower aspect ratios are apparently greater than those at higher aspect ratios. As Rayleigh number increases, the heat transfer rate increases, velocity increases, and the isotherms are no longer orthogonal, they bend. The result indicates that at constant aspect ratio as Rayleigh number increases, Nusselt number increases along the hot wall of the cavity and heat transfer rate also increases, but at constant Rayleigh number as aspect ratio increases, Nusselt number decreases along the same wall.

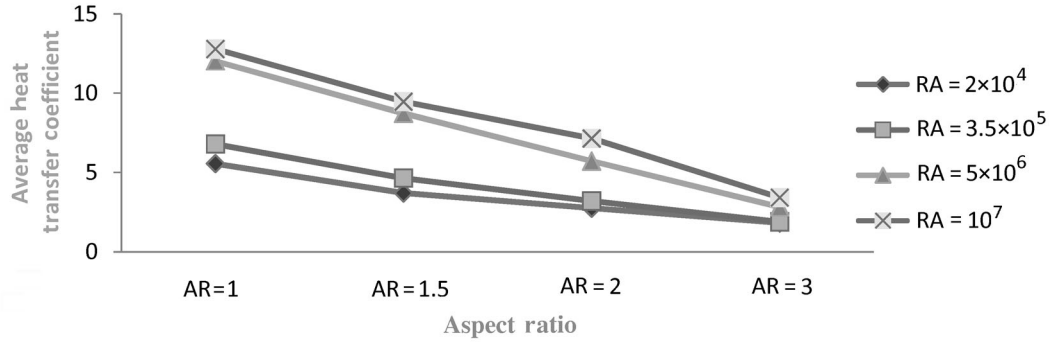

Fig. 11. Variation of average heat transfer coefficient along hot wall of cavity for different aspect ratio and Rayleigh number.

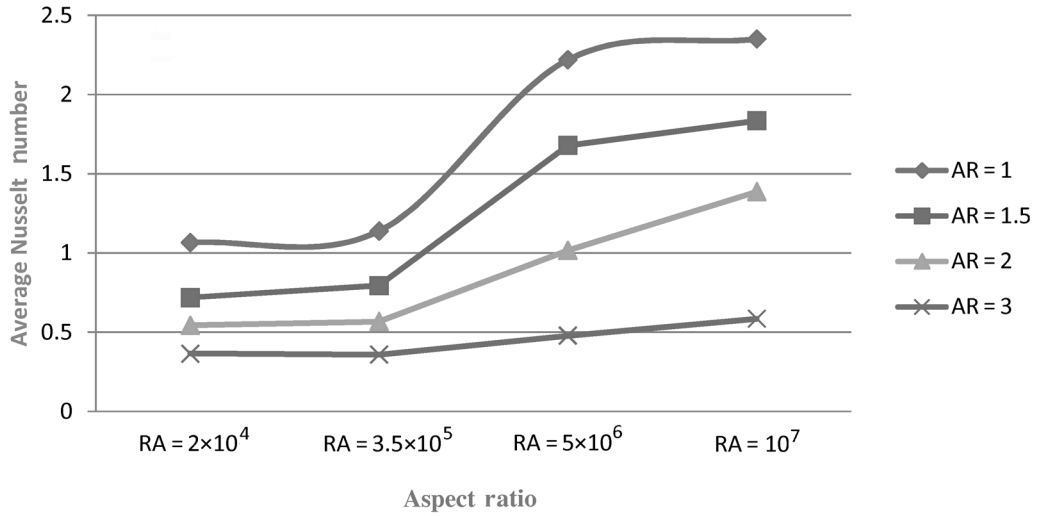

Fig. 12. Variation of average Nusselt number along hot wall of cavity for different aspect ratio and Rayleigh number.

NOTATIONS

g—acceleration due to gravity (ms^{-2})
$alpha$—thermal diffusivity (m^2s^{-1})
κ—thermal conductivity ($Wm^{-1}K^{-1}$)
β—volume expansion coefficient (K^{-1})
L—length of the closed cavity (m)
H—height of the cavity (m)
v—kinematic viscosity (m^2s^{-1}
Pr—Prandtl number
ρ—density ($kg{\cdot}M^{-3}$
T—temperature (K)
ψ—stream function (kg/s)
T_h—temperature of hot bottom wall (K)
μ—dynamic viscosity (Ns/m^2)
T_c—temperature of cold vertical wall (K)
u—x component of velocity

v—y component of velocity
RA—Rayleigh number
ΔT—change in temperature (K)
$\overline{Nu}$—average Nusselt number

REFERENCES

1. De Vahl Davis, G., Natural Convection of Air in a Square Cavity: A Benchmark Numerical Solution, *Int. J. Num. Meth. Fluids,* 1983, vol. 03, pp. 227–248.
2. Freitas, C.J., Street, R.L., Findikakis, A.N., and Koseff, J.R., Numerical Simulation of Three-Dimensional Flow in a Cavity, *Int. J. Num. Meth. Fluids*, 1985, vol. 5, pp. 561–575.
3. Paolucci, S. and Chenoweth, D.R., Natural Convection in Shallow Enclosures with Differentially Heated End Walls, *J. Heat Transfer*, 1988, vol. 110, pp. 625–634.
4. Ostrach, S., *Laminar Flows with Body Force, High Speed Aerodynamics and Jet Propulsion*, vol. 4, Princeton Univ. Press, 1964, pp. 528–718.
5. Ostrach, S., Natural Convection in Enclosures, *Advances in Heat Transfer*, vol. VII, New York: Academic Press, 1972, pp. 161–227.
6. Lo, D.C., Young, D.L, and Tsai, C.C., High Resolution of 2D Natural Convection in Cavity by DQ Method, *J. Comput. Appl. Math.*, 2004, vol. 203, pp. 219–236.
7. Basak, T., Roy, S., and Balakrishnan, A.R., Effects of Thermal Boundary Conditions on Natural Convection Flows within Square Cavity, *Int. J. Heat Mass Transfer*, 2006, vol. 49, pp. 4525–4535.
8. Fusegi, T., Hyun, J.M., and Kuwahara, K., Natural Convection in a Differentially Heated Square Cavity with Internal Heat Generation, *Num. Heat Transfer A*, 1992, vol. 21, pp. 215–229.
9. Lage, J.L. and Benjan, A., The Ra–Pr Domain of Laminar Natural Convection in an Enclosure Heated from the Side, *Num. Heat Transfer A*, 1991, vol. 19, pp. 21–41.
10. Lage, J.L. and Benjan, A., The Resonance of Natural Convection in an Enclosure Heated Periodically from the Side, *Int. J. Heat Mass Transfer*, 1993, vol. 36, pp. 2027–2038.
11. Xia, C. and Murthy, J.Y., Buoyancy-Driven Flow Transitions in Deep Cavities Heated from Below, *ASME Trans. J. Heat Transfer*, 2002, vol. 124, pp. 650–659.
12. November, M. and Nansteel, M.W., Natural Convection in Rectangular Enclosures Heated from Below and Cooled Along One Side, *Int. J. Heat Mass Transfer*, 1987, vol. 30, pp. 2433–2440.
13. Hall, J.D., Bejan, A., and Chaddock, J.B., Transient Natural Convection in Rectangular Enclosure with One Heated Side Wall, *Int. J. Fluid Flow*, 1988, vol. 9, pp. 396–404.
14. Hyun, J.M. and Lee, J.W., Numerical Solutions of Transient Natural Convection in a Square Cavity with Different Side Wall Temperature, *Int. J. Fluid Flow*, 1989, vol. 10, pp. 146–151.
15. Sarris, I.E., Lekakis, I., and Vlachos, N.S., Natural Convection in Rectangular Tanks Heated Locally from Below, *Int. J. Heat Mass Transfer*, 2004, vol. 47, pp. 3549–3563.
16. Corcione, M., Effects of the Thermal Boundary Conditions at the Sidewalls upon Natural Convection in Rectangular Enclosures Heated from Below and Cooled from Above, *Int. J. Therm. Sci.*, 2003, vol. 42, pp. 199–208.
17. Moukalled, F. and Acharya, S., Natural Convection in the Annulus between Concentric Horizontal Circular and Square Cylinders, *AIAA J. Thermophys. Heat Transfer*, 1996, vol. 10, pp. 524–531.
18. Singh, R.K., Sahu, K.B., and Mishra, T.D., Analysis of Heat Transfer and Flow Due to Natural Convection in Air around Heated Square Cylinders of Different Sizes inside an Enclosure, *Int. J. Eng. Res. Appl.*, 2013, vol. 3, pp. 766–771.
19. Wu, W. and Ching, C.Y., The Effect of the Top Wall Temperature on the Laminar Natural Convection in Rectangular Cavities with Different Aspect Ratios, *J. Heat Transfer*, 2009, vol. 131, pp. 1–11.
20. Bose, P.K., Sen, D., Panua, R., and Das, A.K., Numerical Analysis of Laminar Natural Convection in a Quadrantal Cavity with a Solid Adiabatic Fin Attached to the Hot Vertical Wall, *J. Appl. Fluid Mech.*, 2013, vol. 6, pp. 501–510.
21. Hussein, A.K. and Hussain, S.H., Mixed Convection through a Lid-Driven Air-Filled Square Cavity with a Hot Wavy Wall, *Int. J. Mech. Mat. Eng.*, 2010, vol. 5, pp. 222–235.